Desalination and Water Treatment
www.deswater.com

doi: 10.5004/dwt.2017.21192

84 (2017) 255–261
July

Methyl orange removal by a magnetic Fe^0/Fe_3O_4/graphene composite: influencing factors, desulfurization, and mechanism

Shan Chong, Guangming Zhang*, Yucan Liu, Nan Zhang, Ting Huang, Hongchen Wang

School of Environment and Natural Resource, Renmin University of China, 59 Zhongguancun Street, Beijing 100872, China, Tel. +86 10 82502680; emails: zgm@ruc.edu.cn (G. Zhang), chongshan@ruc.edu.cn (S. Chong), lyucan@163.com (Y. Liu), zhangnan0923@163.com (N. Zhang), jason_huangting@163.com (T. Huang), whc@ruc.edu.cn (H. Wang)

Received 16 December 2016; Accepted 5 July 2017

ABSTRACT

A magnetic Fe^0/Fe_3O_4/graphene composite was used to remove methyl orange from water, and its operation was studied in detail. The effects of important parameters were investigated. The results showed that an excellent synergetic effect among Fe^0, Fe_3O_4, and graphene existed in the composite. The composite could remove methyl orange in acidic and alkali conditions as well. In fact, 95.60% of the methyl orange was removed within 20 min. The desulfurization of methyl orange involved cleavage of the azo bond and mineralization of the sulfuric groups; 70% desulfurization efficiency was achieved after 40 min, indicating good detoxification abilities of Fe^0/Fe_3O_4/graphene. The addition of H_2O_2 significantly inhibited the removal efficiency, indicating that reduction was the main role of Fe^0/Fe_3O_4/graphene. X-ray photoelectron spectroscopic analysis showed that O^{2-} groups increased after use, indicating that more lattice oxygen was generated in the form of iron oxides. The increase in Fe^{2+} and decrease in Fe^0 and Fe^{3+} further verified that the oxygen functional groups on graphene were reduced to lattice oxygen in iron oxides by Fe^0. The reaction mechanism was proposed to involve adsorption, surface complexation, cleavage of the azo bond, and mineralization.

Keywords: Fe^0/Fe_3O_4/graphene; Methyl orange; Removal; Reduction; Desulfurization

1. Introduction

Methyl orange is a model azo dye compound, which are widely used in the chemical and textiles industries [1]. Azo dyes discharged in wastewater pose a potential threat to the environment and human health due to their toxicity, non-biodegradation, and carcinogenic effects [2]. Therefore, the removal of azo dyes has been actively studied [3,4]. Due to the stability of the azo structure, traditional biological, physical, and chemical methods have limited effects on the removal of azo dyes [5,6]. Recently, many studies have focused on adsorption and catalytic oxidation technologies for the removal of methyl orange from water. Haldorai and Shim [7] prepared a chitosan/MgO composite for the removal of methyl orange by the adsorption method, and the removal efficiency reached approximately 98% in 5 min. Wang et al. [8] synthesized a FeOOH/CBC composite for the adsorption of methyl orange, and the removal efficiency reached 84.6% in 10 min. Though adsorption method has the advantages of high efficiency and fast removal of methyl orange, it has the disadvantage of concentrating dyes rather than eliminating them, which may create secondary contamination. Catalytic oxidation technology can degrade dyes by the formation of strong oxidizing free radicals. Hassan et al. [9] developed C-doped TiO_2 thin films for the visible-light-induced photocatalytic degradation of methyl orange in water, and the removal efficiency reached 91.89% in 4 h. Wang et al. [10] investigated the ultrasound-assisted catalytic degradation of methyl orange with a Fe_3O_4/polyaniline composite and found that 97.9% of methyl orange was removed in 3 h with an ultrasonic density of 3.3 W/cm^3. Nguyen et al. [11] studied the heterogeneous Fenton oxidation of methyl orange by magnetic Fe_2MO_4 (M:Fe, Mn) activated carbons, and 100%

---

* Corresponding author.

degradation and 59% TOC removal of methyl orange was achieved in 2 h with 1.8×10^{-2} mol/L H_2O_2. However, the problems of low visible-light transmission and high energy and reagent consumption have still not been resolved in the catalytic oxidation process, which restrict its practical application in dyes wastewater treatment. Thus, it is important to develop an efficient and green material and technology to treat dyes wastewater as well as novel approaches to remove azo dyes from water.

The application of zerovalent iron (Fe^0) for pollutants removal has attracted wide attention due to its low cost, low toxicity, and abundance of raw material [12,13]. Fe^0 has significant advantages in wastewater treatment, such as mild reaction conditions and low cost [14]. However, its strong tendency for aggregation under environmental conditions is an important drawback that limits its application in wastewater treatment [15]. Graphene, which has a two-dimensional structure and high surface area [16,17], is an ideal substrate for the chemical deposition of metal particles and has been used as the carrier for metal and metal oxides in pollutants removal [18,19]. The plate-like graphene sheet can decentralize metal particles and enable their uniform dispersion in its layer structure [20,21]. Thus, the combination of graphene and Fe^0 will not only prevent the agglomeration of Fe^0 but also provide good formability. Fe_3O_4, an inverse spinel magnetite, can be easily separated from water with an external magnetic field due to its superparamagnetic property. Therefore, the Fe^0/Fe_3O_4/graphene composite, which combines the features of high reduction ability, anti-aggregation performance, and magnetic property of Fe^0, graphene, and Fe_3O_4 in a single unit, would be an efficient and green material in wastewater treatment.

In a previous study, we synthesized the Fe^0/Fe_3O_4/graphene composite and applied it in dyes wastewater treatment [22]. The composite had a layered structure with Fe crystals highly dispersed in the interlayers of graphene and could be easily separated and redispersed for reuse due to its ferromagnetism. The composite also showed the rapid decolorization of methylene blue, crystal violet, and methyl orange. Since a stable azo structure and organic sulfur exist in the molecular structure of methyl orange ($C_{14}H_{14}N_3NaO_3S$), it is worthwhile to study in detail the removal process and reaction mechanism of methyl orange, especially the transformation of organic sulfur to inorganic sulfur.

In this paper, the synergetic effect of the Fe^0/Fe_3O_4/graphene composite in the methyl orange removal process was detected. The effects of pH, Fe^0/Fe_3O_4/graphene dose, methyl orange concentration, and H_2O_2 addition were investigated in detail. The desulfurization of methyl orange was analyzed to evaluate the degree of mineralization of organic sulfur. The potential mechanism was proposed.

2. Materials and methods

2.1. Materials

Expandable graphite was purchased from Qingdao Taine (China). Methyl orange was purchased from Sinopharm (China). $FeCl_3{\cdot}6H_2O$, $FeSO_4{\cdot}7H_2O$, $KMnO_4$, $NaNO_3$, $NaBH_4$, and NaOH were obtained from Xilong (China). H_2O_2 (30%), $NH_3{\cdot}H_2O$ (28%), HCl (37%), and H_2SO_4 (98%) were supplied by Beijing Chemical (China). N_2 gas was obtained from Beijing Aolin (China).

2.2. Preparation of the Fe^0, Fe_3O_4, and Fe^0/Fe_3O_4/graphene composite

2.2.1. Preparation of the Fe^0/Fe_3O_4/graphene composite

The first step was the synthesis of graphene oxide, and then, the Fe^0/Fe_3O_4/graphene composite was synthesized by a one-step reduction method, as described in an earlier study [22]. Graphene oxide was prepared by following the hydrothermal method [23]. $FeCl_3{\cdot}6H_2O$ and $FeSO_4{\cdot}7H_2O$ solutions were mixed with the prepared graphene oxide under N_2 purging. After 60 min of mechanical stirring, a stoichiometric amount of $NH_3{\cdot}H_2O$ was added to form Fe_3O_4/graphene oxide. $FeSO_4{\cdot}7H_2O$ solution was mixed with the fresh Fe_3O_4/graphene oxide, which were then stirred for 60 min. A stoichiometric amount of $NaBH_4$ was added dropwise, and then, the black material was formed and washed several times until reaching a neutral pH. Fe^0/Fe_3O_4/graphene was separated and dried in a vacuum oven at 50°C for 24 h.

2.2.2. Fe^0 preparation

$FeSO_4{\cdot}7H_2O$ was dissolved in 200 mL of deionized water under vigorous mechanical stirring for 60 min. A stoichiometric amount of $NaBH_4$ was added dropwise and stirred for 60 min. The resulting black material was then washed several times until reaching a neutral pH. Then, Fe^0 was separated by an external magnet and dried in a vacuum oven at 50°C for 24 h.

2.2.3. Fe_3O_4 preparation

$FeCl_3{\cdot}6H_2O$ and $FeSO_4{\cdot}7H_2O$ were dissolved in 400 mL of deionized water under N_2 purging, and then, the solution was under vigorous mechanical stirring for 60 min. A stoichiometric amount of $NH_3{\cdot}H_2O$ was added dropwise and stirred for 60 min. The resulting black material was washed several times until reaching a neutral pH. Then, Fe_3O_4 was separated by an external magnet and dried in a vacuum oven at 50°C for 24 h.

2.3. Experiments

The experiments were conducted as follows. The methyl orange solutions were first adjusted to the desired pH with NaOH and H_2SO_4 solution. Then, a certain dose of Fe^0/Fe_3O_4/graphene was quickly introduced into the solution. Subsequently, the mixed solution was stirred continuously with an electronic stirrer. At set intervals, 1.0 mL of the sample was taken out and filtrated with a 0.45 μm membrane filter. The obtained clear sample was analyzed immediately with a UV spectrometer. Control experiments were also performed under the same conditions.

The determination of methyl orange was performed by a Shimadzu UV2500 spectrometer, and the λ_{max} of methyl orange was 464 nm. The X-ray photoelectron spectra (XPS) of the composites were measured on an Escalab 250Xi spectrometer equipped with an XR6 monochromated X-ray source. SO_4^{2-} was measured by a Dionex ICS-2500 ion chromatograph equipped with a DX-600 ED50A electrochemical detector. The desulfurization efficiency was calculated from the percentage of measured SO_4^{2-} in solution and the theoretical mineralization of organic S.

3. Results and discussion

3.1. Synergetic effects of the Fe^0/Fe_3O_4/graphene composite in methyl orange removal

To evaluate the synergetic effects in Fe^0/Fe_3O_4/graphene composite, the removal efficiency of methyl orange was compared among Fe^0, Fe_3O_4, graphene, and Fe^0/Fe_3O_4/graphene composite. As shown in Fig. 1, graphene removed 18.7% of methyl orange after 40 min, which was mainly attributed to its adsorption activity. Fe_3O_4 achieved only 5% removal, indicating poor oxidation of methyl orange. Fe^0 showed a very quick reaction, and the removal efficiency reached 41% after 1 min but remained below 45% even after 40 min, indicating that reduction was very quick but had limited effect. In contrast, Fe^0/Fe_3O_4/graphene composite showed very good removal efficiency (95.6% within 20 min), and its curve was much smoother than that of Fe^0.

The results suggested that the reduction of Fe^0 played an important role in methyl orange removal. The much higher removal efficiency of the composite clearly showed that synergetic effects existed among Fe^0, Fe_3O_4, and graphene, which could be ascribed to reactions of Fe^0, Fe_3O_4, and graphene in the composite, leading to the reduction and adsorption of methyl orange from aqueous solution [24]. A similar result was found in a study on Cr(VI) removal by Fe^0/Fe_3O_4/graphene. Lv et al. [25] found that the removal efficiency of Cr(VI) was 83.8%, which was much higher than that of the individual components (18.0% for Fe^0, 21.6% for Fe_3O_4, and 23.7% for graphene). Electrons released by Fe^0 spread over the surfaces of graphene and Fe_3O_4, and the adsorbed Cr(VI) ions capture the floating electrons and are reduced to Cr(III). It could be inferred that similar electron transfer behavior occurred in this study; thus, Fe^0/Fe_3O_4/graphene showed a high removal efficiency of methyl orange over a short time. Most processes for methyl orange removal require a large amount of energy and chemicals and involve complex operations, such as photocatalytic [26], sonocatalytic [27], electrocatalytic [28], and heterogeneous Fenton processes [29]. In comparison, this method is very simple, highly effective, and requires no extra energy, which makes it an efficient, green, and sustainable approach in methyl orange wastewater treatment.

3.2. Influencing factors of methyl orange removal by the Fe^0/Fe_3O_4/graphene composite

3.2.1. Effect of initial pH

To investigate the effect of the initial pH on methyl orange removal by Fe^0/Fe_3O_4/graphene, experiments were carried out, and the results are shown in Fig. 2. The initial pH had little effect on the removal of methyl orange. The removal efficiency was slightly higher at pH 3, which may be due to the increased formation of the Fe(II)–methyl orange complex at low pH [30]. Li et al. [31] found that a magnetic hierarchical GOs/Fe_3O_4/PANI composite showed better activity in the removal of methyl orange under acidic conditions. Dadfarnia et al. [32] found that pH 4 provided the highest removal efficiency of methyl red using an iron-based metal organic framework loaded with iron oxide nanoparticles; and the pH was proposed to affect the surface charge of the material and the degree of ionization of the organic pollutants. In this study, pH was not a limiting factor, Fe^0/Fe_3O_4/graphene had good activity under acidic, neutral, and alkaline conditions, which is desirable for industrial application since the pH of most dye wastewater is in the range of 6–10 [24]. The neutral pH of 7 was used in the following experiments.

3.2.2. Effect of Fe^0/Fe_3O_4/graphene dose

The reagent concentration is a determinative parameter in chemical reactions. The effect of the Fe^0/Fe_3O_4/graphene

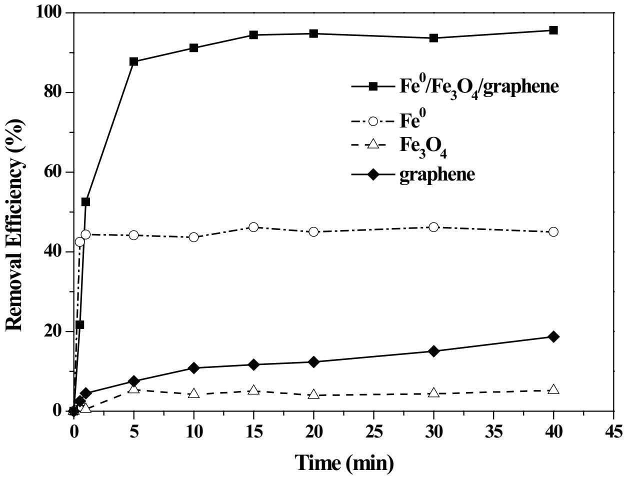

Fig. 1. Removal of methyl orange by various reagents. Experimental conditions: [methyl orange] = 50 mg/L, pH = 7, and [reagent dose] = 1.0 g/L.

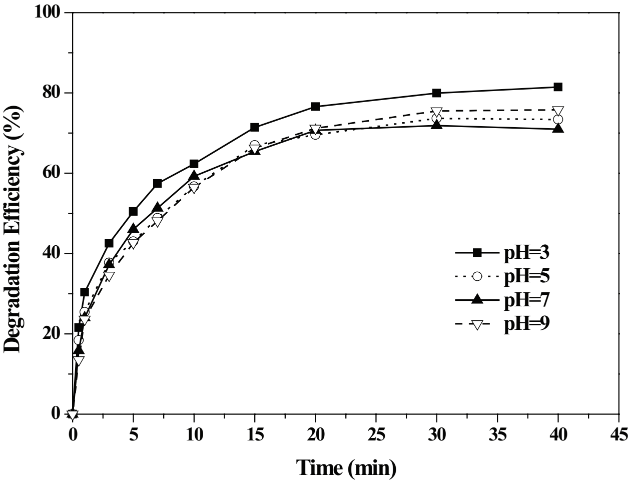

Fig. 2. Effect of initial pH on methyl orange removal by Fe^0/Fe_3O_4/graphene. Experimental conditions: [methyl orange] = 50 mg/L and Fe^0/Fe_3O_4/graphene = 0.4 g/L.

dose was investigated, and the results are shown in Fig. 3. The removal efficiency of methyl orange increased significantly with the composite dose increasing from 0.1 to 1.0 g/L. Since the reaction occurred at the interface of the composite and water, a higher composite addition led to a higher amount of adsorptive and reactive sites. In addition, the composite dose might be correlated with the amount of electrons transferred in the reaction, which plays an important role in redox processes [25]. A further increase in the composite dose was unnecessary since the removal efficiency was already over 95%.

3.2.3. *Effect of initial concentration of methyl orange*

The initial methyl orange concentration also influences its removal, and the results are summarized in Fig. 4. The removal efficiency of methyl orange first increased and then decreased with the initial concentration increasing from 10 to 80 mg/L. In general, the reaction was benefitted by a higher reagent concentration, as more methyl orange molecules aggregated at the active sites and facilitated electron transfer. Su et al. [33] also observed a similar phenomenon in the degradation of amoxicillin using sulfate radicals under ultrasound irradiation. However, excess methyl orange molecules would cover the active sites and hinder electron transfer, which is detrimental to the reaction. The highest removal efficiency of 95.6% was achieved at 50 mg/L.

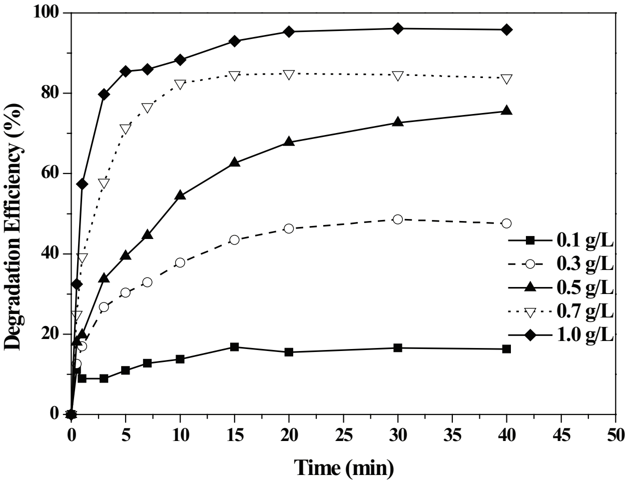

Fig. 3. Effect of Fe^0/Fe_3O_4/graphene dose on methyl orange removal. Experimental conditions: [methyl orange] = 50 mg/L and pH = 7.

3.2.4. *Effect of H_2O_2 addition*

Studies have shown that a mixture of various Fe-containing materials and H_2O_2 can form a heterogeneous Fenton-like system that shows excellent degradation ability for organics in water [34,35]. Thus, we added H_2O_2 to the Fe^0/Fe_3O_4/graphene system in an attempt to enhance its efficiency, and the results are shown in Fig. 5. Clearly, H_2O_2 was ineffective on methyl orange (only 1.8% after 40 min). The addition of H_2O_2 sharply decreased the methyl removal efficiency to 18.7%, showing that H_2O_2 significantly inhibited the activity of Fe^0/Fe_3O_4/graphene. This behavior was mainly attributed to the redox reaction between the composite and H_2O_2, which weakened the reduction capability of the composite. These results indicated that the reduction of Fe^0/Fe_3O_4/graphene dominated the removal process.

3.3. *Desulfurization of methyl orange by Fe^0/Fe_3O_4/graphene*

Since organic sulfur compounds are highly toxic and stable in the environment, it is important to transform organic sulfur into inorganic sulfur to reduce its toxicity. Generally, sulfate ions (SO_4^{2-}) are the mineralization product of organic sulfur compounds. Thus, to investigate the desulfurization of methyl orange by Fe^0/Fe_3O_4/graphene, SO_4^{2-} generation was measured, and the results are shown in Fig. 6. Some useful insights into the removal process of methyl orange were obtained from the trend of the desulfurization curve.

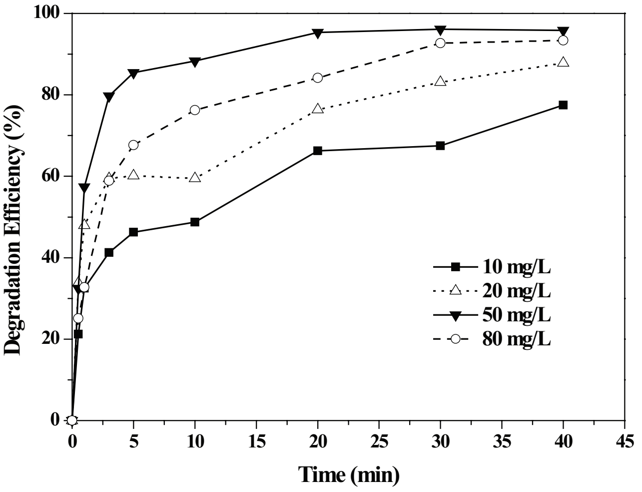

Fig. 4. Effect of initial concentration of methyl orange on its removal. Experimental conditions: pH = 7 and Fe^0/Fe_3O_4/graphene = 1.0 g/L.

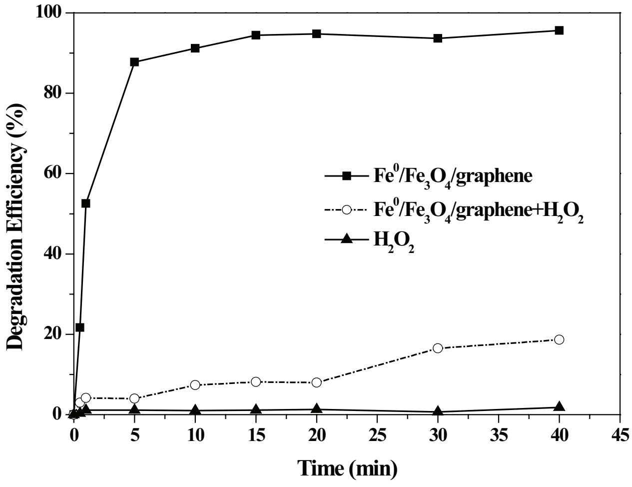

Fig. 5. Effect of H_2O_2 addition on methyl orange removal. Experimental conditions: [methyl orange] = 50 mg/L, pH = 7, Fe^0/Fe_3O_4/graphene = 1.0 g/L, and [H_2O_2] = 200 mmol/L.

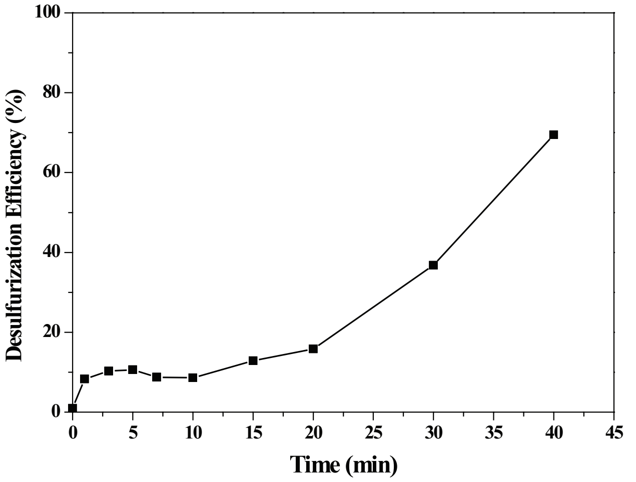

Fig. 6. Desulfurization of methyl orange by Fe^0/Fe_3O_4/graphene. Experimental conditions: [methyl orange] = 50 mg/L, pH = 7, and Fe^0/Fe_3O_4/graphene = 1.0 g/L.

The quick but small increase of SO_4^{2-} in the first 1 min was attributed to residues from preparation. Then, the SO_4^{2-} concentration stabilized from 1 to 10 min, suggesting that no sulfuric groups in methyl orange were transformed to SO_4^{2-} ions at this stage. The SO_4^{2-} concentration increased slowly from 10 to 20 min, and at the same time, 95% of methyl orange was removed within 20 min, suggesting that most methyl orange molecules were transformed to S-containing intermediates. After 20 min, the desulfurization efficiency increased rapidly, indicating the desulfurization of the intermediates occurred. The desulfurization efficiency achieved 70% after 40 min, indicating that most of the organic sulfur in methyl orange was transformed to inorganic sulfur ions during the removal process. This behavior is desirable since desulfurization signifies detoxification.

Based on the above analysis, methyl orange removal by Fe^0/Fe_3O_4/graphene included two steps. The first step was the cleavage of the azo bond, accompanied by the formation of new products, which is in accordance with previous studies [36]. The second step was the desulfurization of intermediates, which undergo mineralization of the sulfuric groups and ring cleavage and eventually transform into inorganic materials, such as SO_4^{2-}, CO_2, and H_2O.

3.4. XPS analysis

To further study the reaction mechanism of Fe^0/Fe_3O_4/graphene and methyl orange, the fresh and used composites were examined by XPS. The XPS of the fresh and used Fe^0/Fe_3O_4/graphene composites are shown in Fig. 7(a). The photoelectron peaks demonstrated the presence of C, O, and Fe elements on the surface of the fresh and used composites. The binding energies at 285, 531, 710, and 725 eV were attributed to C 1s, O 1s, Fe $2p_{3/2}$, and Fe $2p_{1/2}$, respectively.

The high-resolution scan of C 1s is shown in Fig. 7(b). The C 1s spectra could be deconvoluted into three peaks: (1) non-oxygenated carbon (C–C, 284.8 eV), (2) carbon in C–O (285.6 eV), and (3) carboxylate carbon (O–C=O, 288.8 eV). The content percentages of the C–C, C–O, and O–C=O groups were 47.02%, 41.64%, and 11.34% in the fresh sample, respectively. After reaction, the values changed to 46.61%, 31.95%, and 21.44%, respectively. The increase in O–C=O groups and decrease in C–O groups suggested that graphene was gradually oxidized to graphene oxide after reaction.

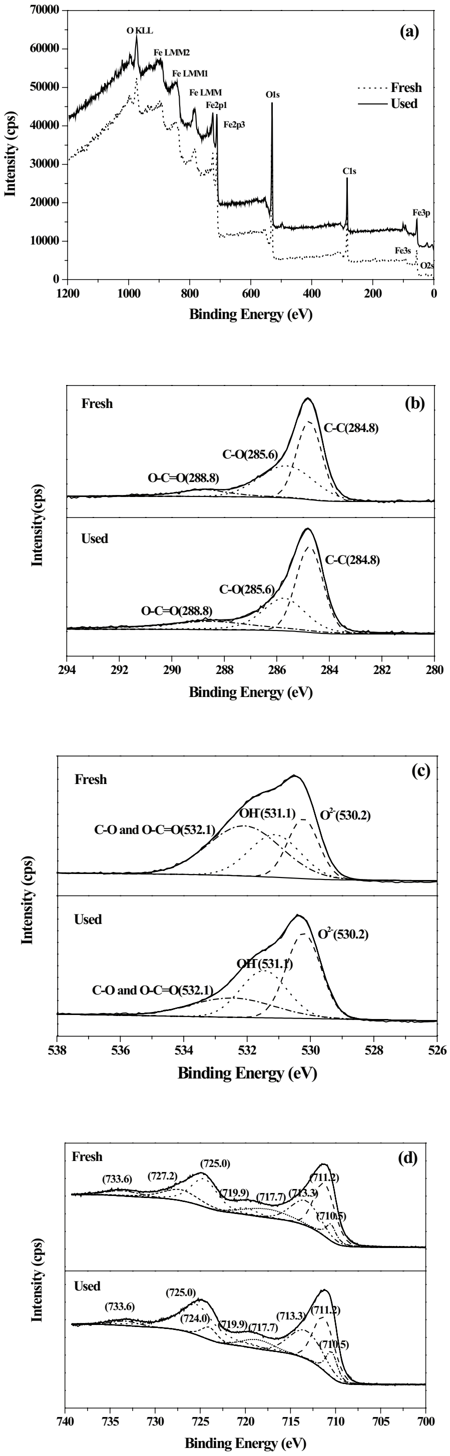

Fig. 7. The XPS of fresh and used Fe^0/Fe_3O_4/graphene: (a) survey scan, (b) C 1s, (c) O 1s, and (d) Fe 2p energy regions.

The high-resolution scan of O 1s is shown in Fig. 7(c). Deconvolution of the O 1s peak showed three peaks at 530.2, 531.1, and 532.1 eV, corresponding to O^{2-}, OH^-, C–O, and O–C=O groups, respectively [37]. The content percentages of O^{2-}, OH^-, C–O, and O–C=O groups were 24.11%, 28.40%, and 47.49% in the fresh composite, respectively. After reaction, the values were 43.44%, 32.51%, and 24.05%, respectively. The increase of O^{2-} groups indicated that more lattice oxygen was generated in the form of iron oxides after use. The decrease of C–O and O–C=O groups indicated that O on the surface of graphene was transformed to other forms in the composite. According to the C 1s and O 1s analyses, it was proposed that oxygen functional groups on graphene were reduced to lattice oxygen in iron oxides by Fe^0.

The high-resolution scan of Fe 2p region is shown in Fig. 7(d). The binding energy at 719.9 eV can be ascribed to Fe^0 $2p_{1/2}$, indicating that Fe^0 existed on the surface of Fe^0/Fe_3O_4/graphene [38]. The binding energy at 710.5 eV, with satellites at 713.3 and 727.2 eV, can be ascribed to Fe^{2+}, while the binding energy at 725.0 eV, with satellites at 733.6 and 717.7 eV, can be ascribed to Fe^{3+} in iron oxides [39]. The content percentages of Fe^0, Fe^{2+}, and Fe^{3+} were 4.25%, 35.65%, and 60.10% in the fresh composite, respectively. After reaction, the percentages were 2.49%, 59.60%, and 37.91%, respectively. The increase of Fe^{2+} and decrease of Fe^0 and Fe^{3+} suggested that Fe^0 was oxidized and Fe^{3+} was reduced to Fe^{2+} on the surface of the composite. These results are in accordance with the lattice oxygen conclusions in the analysis of the O 1s region.

3.5. Potential reaction mechanism

The above results suggest that the desulfurization of methyl orange involves the cleavage of the azo bond and mineralization of the sulfuric groups. Graphene in the composite was gradually oxidized to graphene oxide, and more lattice oxygen was generated in the form of iron oxides after reaction. The increase of Fe^{2+} and decrease of Fe^0 and Fe^{3+} further verified that the oxygen functional groups on graphene were reduced to lattice oxygen in iron oxides by Fe^0. Thus, it can be concluded that synergetic effects among Fe^0, Fe_3O_4, and graphene existed in the composite.

The mechanism for the removal of methyl orange by Fe^0/Fe_3O_4/graphene was proposed based on the above analysis (Fig. 8). The process included the following steps: adsorption, surface complexation, cleavage of the azo bond, and mineralization. Methyl orange molecules were first adsorbed onto the surface of Fe^0/Fe_3O_4/graphene due to the adsorption activity of graphene. At the same time, Fe^0 was oxidized by oxygen in water or Fe^{3+} in Fe_3O_4 to generate active Fe^{2+} on the surface. Since both Fe^{2+} and Fe^{3+} are accommodated in Fe_3O_4, Fe^0/Fe_3O_4/graphene can undergo numerous successive redox cycles during the process. The synergetic effect of Fe^0, Fe_3O_4, and graphene in the composite can accelerate electron transfer and thus improve the reaction rate. As Fe^{2+} was generated continuously on the surface of the composite, the chelate complex of Fe(II)–methyl orange was formed due to the electrostatic interaction of Fe^{2+} and the azo bond. Then, H radicals generated by reaction of Fe^0 and H_2O can cause the azo bond to break [30]. Finally, methyl orange was reduced to small molecules through azo bond cleavage, and sulfuric groups in the intermediates were transformed to inorganic sulfate ions.

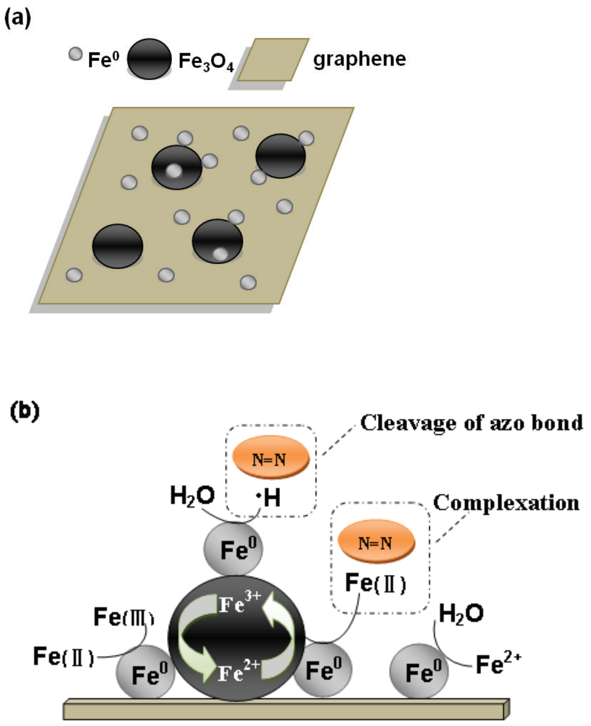

Fig. 8. Schematic of dye removal process by Fe^0/Fe_3O_4/graphene: (a) general view and (b) reaction mechanism.

4. Conclusions

The removal of methyl orange from aqueous solution by a magnetic Fe^0/Fe_3O_4/graphene composite was investigated in detail. Compared with graphene, Fe_3O_4, and Fe^0 alone, the composite possessed the highest activity, indicating an excellent synergetic effect. The optimum conditions of pH, dose, and initial concentration were pH 7, 1.0 g/L, and 50 mg/L, respectively. The removal efficiency achieved 95.6% within 20 min, and approximately 70% of organic S was transformed into SO_4^{2-} within 40 min. The removal process was deduced to include the following steps: adsorption, surface complexation, cleavage of the azo bond, and mineralization. The synergetic effect of Fe^0, Fe_3O_4, and graphene in the composite accelerates electron transfer, and the reduction of the composite played a key role in the removal process.

Acknowledgment

The authors are thankful for the support from the Beijing Natural Science Foundation (817202) and the Beijing Municipal Science and Technology Commission (Z151100001415005).

References

[1] J. Guo, D.J. Jiang, Y. Wu, P. Zhou, Y.Q. Lan, Degradation of methyl orange by Zn(0) assisted with silica gel, J. Hazard. Mater., 194 (2011) 290–296.
[2] H. Zhao, G. Zhang, Q. Zhang, MnO_2/CeO_2 for catalytic ultrasonic degradation of methyl orange, Ultrason. Sonochem., 21 (2014) 991–996.

[3] Z. Eren, Degradation of an azo dye with homogeneous and heterogeneous catalysts by sonophotolysis, Clean Soil Air Water, 40 (2012) 1284–1289.

[4] J. Wang, T. Ma, Z.H. Zhang, X.D. Zhang, Y.F. Jiang, Z.J. Pan, F.Y. Wen, P.L. Kang, P. Zhang, Investigation on the sonocatalytic degradation of methyl orange in the presence of nanometer anatase and rutile TiO_2 powders and comparison of their sonocatalytic activities, Desalination, 195 (2006) 294–305.

[5] S. Netpradit, P. Thiravetyan, S. Towprayoon, Adsorption of three azo reactive dyes by metal hydroxide sludge: effect of temperature, pH, and electrolytes, J. Colloid Interface Sci., 270 (2004) 255–261.

[6] S. Padamavathy, S. Sandhya, K. Swaminathan, Y.V. Subrahmanyam, S.N. Kaul, Comparison of decolorization of reactive azo dyes by microorganisms isolated from various sources, J. Environ. Sci. China, 15 (2003) 628–632.

[7] Y. Haldorai, J.J. Shim, An efficient removal of methyl orange dye from aqueous solution by adsorption onto chitosan/MgO composite: a novel reusable adsorbent, Appl. Surf. Sci., 292 (2014) 447–453.

[8] Z. Wang, Y. Ma, H. He, C. Pei, P. He, A novel reusable nanocomposite: FeOOH/CBC and its adsorptive property for methyl orange, Appl. Surf. Sci., 332 (2015) 456–462.

[9] M.E. Hassan, L. Cong, G. Liu, D. Zhu, J. Cai, Synthesis and characterization of C-doped TiO_2 thin films for visible-light-induced photocatalytic degradation of methyl orange, Appl. Surf. Sci., 294 (2014) 89–94.

[10] Y. Wang, L. Gai, W. Ma, H. Jiang, X. Peng, L. Zhao, ultrasound-assisted catalytic degradation of methyl orange with Fe_3O_4/polyaniline in near neutral solution, Ind. Eng. Chem. Res., 54 (2015) 2279–2289.

[11] T.D. Nguyen, N.H. Phan, M.H. Do, K.T. Ngo, Magnetic Fe(2)MO(4) (M:Fe, Mn) activated carbons: fabrication, characterization and heterogeneous Fenton oxidation of methyl orange, J. Hazard. Mater., 185 (2011) 653–661.

[12] B.H. Moon, Y.B. Park, K.H. Park, Fenton oxidation of Orange II by pre-reduction using nanoscale zero-valent iron, Desalination, 268 (2011) 249–252.

[13] H.Y. Shu, M.C. Chang, H.H. Yu, W.H. Chen, Reduction of an azo dye Acid Black 24 solution using synthesized nanoscale zerovalent iron particles, J. Colloid Interface Sci., 314 (2007) 89–97.

[14] X. Ling, J. Li, W. Zhu, Y. Zhu, X. Sun, J. Shen, W. Han, L. Wang, Synthesis of nanoscale zero-valent iron/ordered mesoporous carbon for adsorption and synergistic reduction of nitrobenzene, Chemosphere, 87 (2012) 655–660.

[15] X. Wang, P. Wang, J. Ma, H. Liu, P. Ning, Synthesis, characterization, and reactivity of cellulose modified nano zero-valent iron for dye discoloration, Appl. Surf. Sci., 345 (2015) 57–66.

[16] M.D. Stoller, Graphene-based ultracapacitors, Nano Lett., 8 (2008) 3498–3502.

[17] D. Lu, Y. Zhang, S. Lin, L. Wang, C. Wang, Synthesis of magnetic $ZnFe_2O_4$/graphene composite and its application in photocatalytic degradation of dyes, J. Alloys Compd., 579 (2013) 336–342.

[18] C. Wang, H. Luo, Z. Zhang, Y. Wu, J. Zhang, S. Chen, Removal of As(III) and As(V) from aqueous solutions using nanoscale zero valent iron-reduced graphite oxide modified composites, J. Hazard. Mater., 268 (2014) 124–131.

[19] P. Roy, A.P. Periasamy, C.T. Liang, H.T. Chang, Synthesis of graphene-ZnO-Au nanocomposites for efficient photocatalytic reduction of nitrobenzene, Environ. Sci. Technol., 47 (2013) 6688–6695.

[20] Y.W. Liu, M.X. Guan, L. Feng, S.L. Deng, J.F. Bao, S.Y. Xie, Z. Chen, R.B. Huang, L.S. Zheng, Facile and straightforward synthesis of superparamagnetic reduced graphene oxide-Fe_3O_4 hybrid composite by a solvothermal reaction, Nanotechnology, 24 (2013) 025604.

[21] X. Shen, J. Wu, S. Bai, H. Zhou, One-pot solvothermal syntheses and magnetic properties of graphene-based magnetic nanocomposites, J. Alloys Compd., 506 (2010) 136–140.

[22] S. Chong, G. Zhang, H. Tian, H. Zhao, Rapid degradation of dyes in water by magnetic Fe^0/Fe_3O_4/graphene composites, J. Environ. Sci., 44 (2016) 148–157.

[23] C.L. Bao, L. Song, W.Y. Xing, B.H. Yuan, C.A. Wilkie, J.L. Huang, Y.Q. Guo, Y. Hu, Preparation of graphene by pressurized oxidation and multiplex reduction and its polymer nanocomposites by masterbatch-based melt blending, J. Mater. Chem., 22 (2012) 6088–6096.

[24] J. Fan, Y. Guo, J. Wang, M. Fan, Rapid decolorization of azo dye methyl orange in aqueous solution by nanoscale zerovalent iron particles, J. Hazard. Mater., 166 (2009) 904–910.

[25] X. Lv, X. Xue, G. Jiang, D. Wu, T. Sheng, H. Zhou, X. Xu, Nanoscale zero-valent iron (nZVI) assembled on magnetic Fe_3O_4/graphene for chromium (VI) removal from aqueous solution, J. Colloid Interface Sci., 417 (2014) 51–59.

[26] S. Morales-Torres, L.M. Pastrana-Martinez, J.L. Figueiredo, J.L. Faria, A.M.T. Silva, Graphene oxide-P25 photocatalysts for degradation of diphenhydramine pharmaceutical and methyl orange dye, Appl. Surf. Sci., 275 (2013) 361–368.

[27] Y. Iida, T. Kozuka, T. Tuziuti, K. Yasui, Sonochemically enhanced adsorption and degradation of methyl orange with aluminas, Ultrasonics, 42 (2004) 635–639.

[28] W. He, X. Yan, H. Ma, J. Yu, J. Wang, X. Huang, Degradation of methyl orange by electro-Fenton-like process in the presence of chloride ion, Desal. Wat. Treat., 51 (2013) 6562–6571.

[29] Z. Xu, J. Liang, L. Zhou, Photo-Fenton-like degradation of azo dye methyl orange using synthetic ammonium and hydronium jarosite, J. Alloys Compd., 546 (2013) 112–118.

[30] Z.X. Chen, X.Y. Jin, Z. Chen, M. Megharaj, R. Naidu, Removal of methyl orange from aqueous solution using bentonite-supported nanoscale zero-valent iron, J. Colloid Interface Sci., 363 (2011) 601–607.

[31] J. Li, Z. Shao, C. Chen, X. Wang, Hierarchical GOs/Fe_3O_4/PANI magnetic composites as adsorbent for ionic dye pollution treatment, RSC Adv., 4 (2014) 38192–38198.

[32] S. Dadfarnia, A.M.H. Shabani, S.E. Moradi, S. Emami, Methyl red removal from water by iron based metal-organic frameworks loaded onto iron oxide nanoparticle adsorbent, Appl. Surf. Sci., 330 (2015) 85–93.

[33] S. Su, W. Guo, C. Yi, Y. Leng, Z. Ma, Degradation of amoxicillin in aqueous solution using sulphate radicals under ultrasound irradiation, Ultrason. Sonochem., 19 (2012) 469–474.

[34] N.A. Zubir, C. Yacou, J. Motuzas, X. Zhang, J.C. Diniz da Costa, Structural and functional investigation of graphene oxide–Fe_3O_4 nanocomposites for the heterogeneous Fenton-like reaction, Sci. Rep., 4 (2014) 4594.

[35] Y.C. Lee, S.J. Chang, M.H. Choi, T.J. Jeon, T. Ryu, Y.S. Huh, Self-assembled graphene oxide with organo-building blocks of Fe-aminoclay for heterogeneous Fenton-like reaction at near-neutral pH: a batch experiment, Appl. Catal., B, 142 (2013) 494–503.

[36] S. Luo, P. Qin, J. Shao, L. Peng, Q. Zeng, J.D. Gu, Synthesis of reactive nanoscale zero valent iron using rectorite supports and its application for Orange II removal, Chem. Eng. J., 223 (2013) 1–7.

[37] Y. Xi, Z. Sun, T. Hreid, G.A. Ayoko, R.L. Frost, Bisphenol A degradation enhanced by air bubbles via advanced oxidation using in situ generated ferrous ions from nano zero-valent iron/palygorskite composite materials, Chem. Eng. J., 247 (2014) 66–74.

[38] G. Bhargava, I. Gouzman, C.M. Chun, T.A. Ramanarayanan, S.L. Bernasek, Characterization of the “native” surface thin film on pure polycrystalline iron: a high resolution XPS and TEM study, Appl. Surf. Sci., 253 (2007) 4322–4329.

[39] H. Zhao, Y. Wang, Y. Wang, T. Cao, G. Zhao, Electro-Fenton oxidation of pesticides with a novel Fe_3O_4@Fe_2O_3/activated carbon aerogel cathode: high activity, wide pH range and catalytic mechanism, Appl. Catal., B, 125 (2012) 120–127.